

ABSTRACT

Title of dissertation: Measuring topology of BECs
in a synthetic dimensions lattice

Dina Genkina
Doctor of Philosophy, 2018

Dissertation directed by: Professor Ian Spielman
Department of Physics

Measuring topology of BECs in a synthetic dimensions lattice

by

Dina Genkina

Dissertation submitted to the Faculty of the Graduate School of the
University of Maryland, College Park in partial fulfillment
of the requirements for the degree of
Doctor of Philosophy
2018

Advisory Committee:
Professor Ian Spielman, Chair/Advisor

© Copyright by
Dina Genkina
2018

Chapter 6: Synthetic Magnetic Fields in Synthetic Dimensions

In condensed matter, 2-D systems in high fields have proved to be of great technological use and scientific interest. The integer quantum Hall effect (IQHE) [1], with its quantized Hall resistance, had given rise to an ultra-precise standard for resistivity. It was also one of the first examples of topology playing an important role in physics—the precise quantization of the Hall conductance is guaranteed by the non-trivial topology of the system [2]. This quantizes the magnetic flux into flux quanta of $\Phi_0 = 2\pi\hbar/e$, where e is the electron charge, and leads to a new ‘plateau’ in the resistivity when an additional quantum of flux is threaded through the system.

In the IQHE system, the underlying lattice structure of metal is effectively washed out—the magnetic flux per individual lattice plaquette is negligible. However, new physics arises when the magnetic flux per plaquette is increased to some non-negligible fraction of the flux quantum, giving rise to the Hofstadter butterfly [3]. These regimes are hard to reach experimentally, since the typical plaquette size in crystalline material is of order a square angstrom, and the magnetic field necessary to thread create a magnetic flux of Φ_0 through such a narrow area is of order $\approx 10^4$ Tesla, not accessible with current technology.

Several platforms have, however, reached the Hofstadter regime by engineering systems with large effective plaquette size, in engineered materials [4, 5], and in atomic [6–11] and optical [12] settings. Here, we use the approach of synthetic dimensions [13] to reach the Hofstadter regime. We demonstrate the non-trivial topology of the system created, and use it to image skipping orbits at the edge of

the 2-D system—a hallmark of 2-D electron systems in a semiclassical treatment.

The work described in this chapter was published in [14].

6.1 Synthetic dimensions setup

Any internal degree of freedom can be thought of as a synthetic dimension—the different internal states can be treated as sites along this synthetic direction. As long as there is some sense of distance along this direction, i.e. some of the internal states are 'nearest neighbors' while others are not, this is a meaningful treatment. In our case an effective 2-D lattice is formed by sites formed by a 1-D optical lattice along a 'real' direction, here \mathbf{e}_x , and the atom's spin states forming sites along a 'synthetic' direction, \mathbf{e}_s .

The experimental setup for this system is schematically represented in 1a. The BEC is subject to a 1-D optical lattice, formed by a retro-reflected beam of $\lambda_L = 1064nm$ along \mathbf{e}_x . A bias magnetic field B_0 along \mathbf{e}_z separates the different spin states. The spin states can be thought of as sites along a synthetic dimension even without any coupling field. However, only once a coupling field is present do they acquire a sense of distance. We couple them via rf or Raman coupling, which only couples adjacent spin states. The Raman beams illuminating the atoms are along the same \mathbf{e}_x direction as the 1-D optical lattice. The rf field has components both along the \mathbf{e}_x and \mathbf{e}_y .

Figure 1b sketches out the effective 2-D lattice created. Here, we have labelled the lattice sites along the 'real' direction \mathbf{e}_x by site index j . In the tight binding approximation, we can describe a lattice hopping between adjacent sites with tunneling amplitude t_x . Similarly, the sites along the 'synthetic' dimension are labelled by site index m (identical to spin projection quantum number m_F), and the rf or Raman coupling here plays the role of a tunneling amplitude t_s . In the case of rf coupling, there is no momentum kick associated with spin exchange, and both t_x

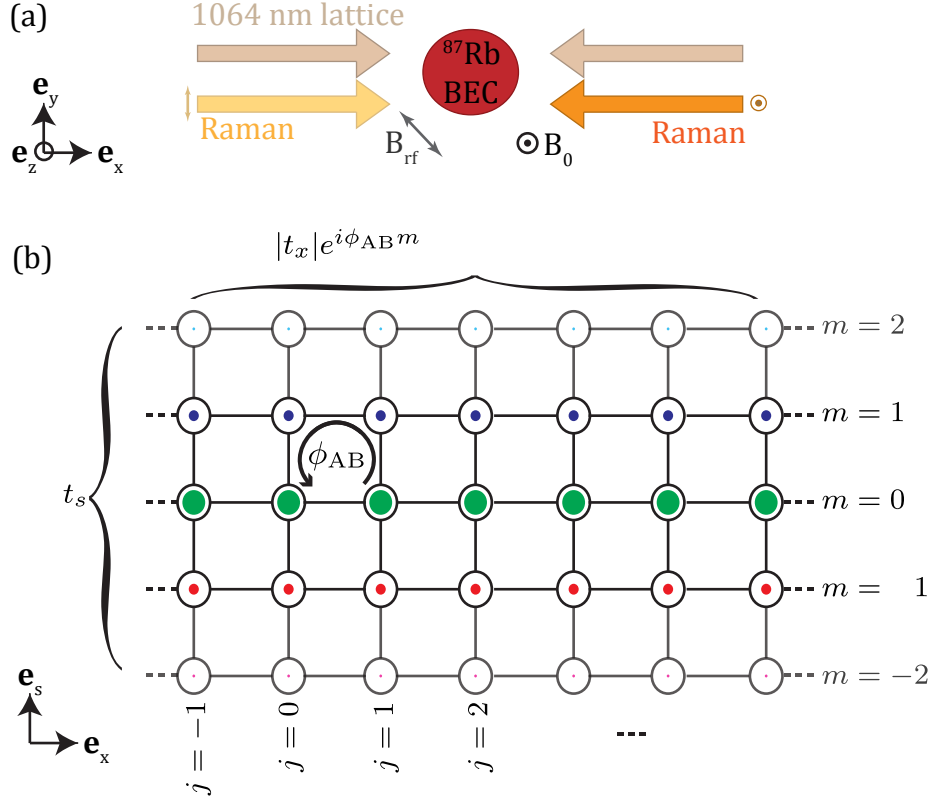


Figure 1: Setup of effective 2-D lattice. (a) Beam geometry. The BEC is subject to a bias magnetic field B_0 in the \mathbf{e}_z direction. The 1-D lattice beam and Raman beams are both along the \mathbf{e}_x direction, and the rf field can be applied with projections onto both the \mathbf{e}_x and \mathbf{e}_y . (b) Schematic of the effective 2-D lattice. Sites along \mathbf{e}_x are formed by the 1-D optical lattice and labelled by site number j . Sites along the synthetic direction \mathbf{e}_s are formed by the spin states: 3 sites for atoms in the $F = 1$ manifold and 5 sites for atoms in $F = 2$. These sites are labelled by m . Raman transitions induce a phase shift, which can be gauge transformed into a tunneling phase along the \mathbf{e}_x direction. This leads to a net phase when hopping around a single lattice plaquette of ϕ_{AB} .

and t_s are real.

In the case of Raman coupling, however, there is a momentum kick of $2k_R$ associated with every spin transfer, and therefore a phase factor of $\exp(2ik_R x)$ with every spin 'tunneling' event. Since position x is set by the 1-D lattice, $x_j = j\lambda_L/2 = j\pi/k_L$, and the space dependent phase factor is $\exp(2\pi i k_R/k_L j)$. An absolute phase change in the wavefunction is not meaningful. However, a phase acquired when going around a plaquette and coming back to the same place is meaningful, as one could imagine one atom staying at the same site and the other going around a plaquette and coming back to detect the phase difference. In this setup, the phases acquired while going around a single plaquette are, starting at some lattice site $|j, m\rangle$, are: 0 (for tunneling right to $|j+1, m\rangle$), $2\pi i k_R/k_L(j+1)$ (for tunneling up to $|j+1, m+1\rangle$), 0 (for tunneling left to $|j, m+1\rangle$) and $-2\pi i k_R/k_L j$ (for tunneling back down to $|j, m\rangle$). The total phase acquired is thus $\phi_{AB} = 2\pi k_R/k_L$, independent of the starting lattice site. Since the absolute phase does not matter and only the value of ϕ_{AB} , we can perform a phase transformation that shifts the tunneling phase onto the spatial direction, defining $t_x = |t_x|\exp(i\phi_{AB}m)$ and $t_s = |t_s|$, as labelled in Figure 1b.

To see how this phase implies an effective magnetic field, we draw an analogy to the Aharonov-Bohm effect [15, 16] from quantum mechanics. In this effect, consider an infinite solenoid with an electric current running through it. The magnetic field B in this setup exists only inside the solenoid, while the magnetic vector potential persists outside the solenoid. However, if two electrons are sent on a trajectory around the solenoid, even though they never pass through any magnetic field, they nevertheless acquire a relative phase that can be detected by interfering them with each other. This relative phase is given by $\phi_{AB} = 2\pi\Phi/\Phi_0$, where $\Phi = B * A$ is the magnetic flux through the solenoid (A is the area pierced by the magnetic field) and $\Phi_0 = h/e$ is the flux quantum, with e the electron charge. Since in our system,

the atoms acquire a phase when they perform a closed loop around a single lattice plaquette. Therefore, they behave as though there was an infinite solenoid piercing each plaquette with a magnetic field going through it, and the flux per plaquette in units of the flux quantum is $\Phi/\Phi_0 = \phi_{AB}/2\pi = k_R/k_L$.

6.2 Hamiltonian of the effective 2-D system

Figure: Band structure, $F=1$ and $F=2$, with and without Raman coupling

par1: Write out full Hamiltonian

par2: Talk about band structure, periodic and spin dependent

par3: How we calibrate the synthetic dimensions system by pulsing

Figure: example TOF images, pulsing experiments for $F=1$ and $F=2$

par4: Write out tight binding version, explain how closely it applies. Figure: fits for effective tunneling amplitudes?

6.3 Eigenstates of the synthetic 2-D lattice

par1: 'Edge' and 'bulk' states of electrons in a magnetic field

par2: Explain loading procedure for adiabatic states

par3: Explain figure, magnetic length

6.4 Observation of skipping orbits

par1: Skipping orbits in 2-D electrons in a magnetic fields

par2: Experimental sequence for skipping orbits measurement

par3: How position is calculated from integrating velocity as a function of time. Explain figure

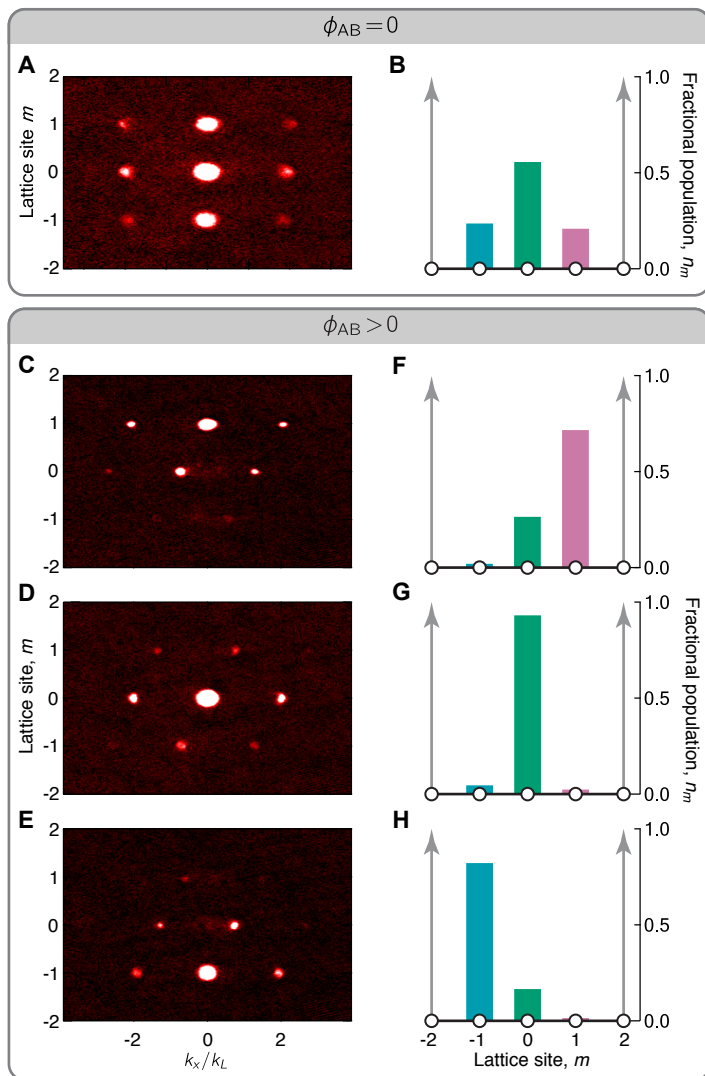


Figure 2:

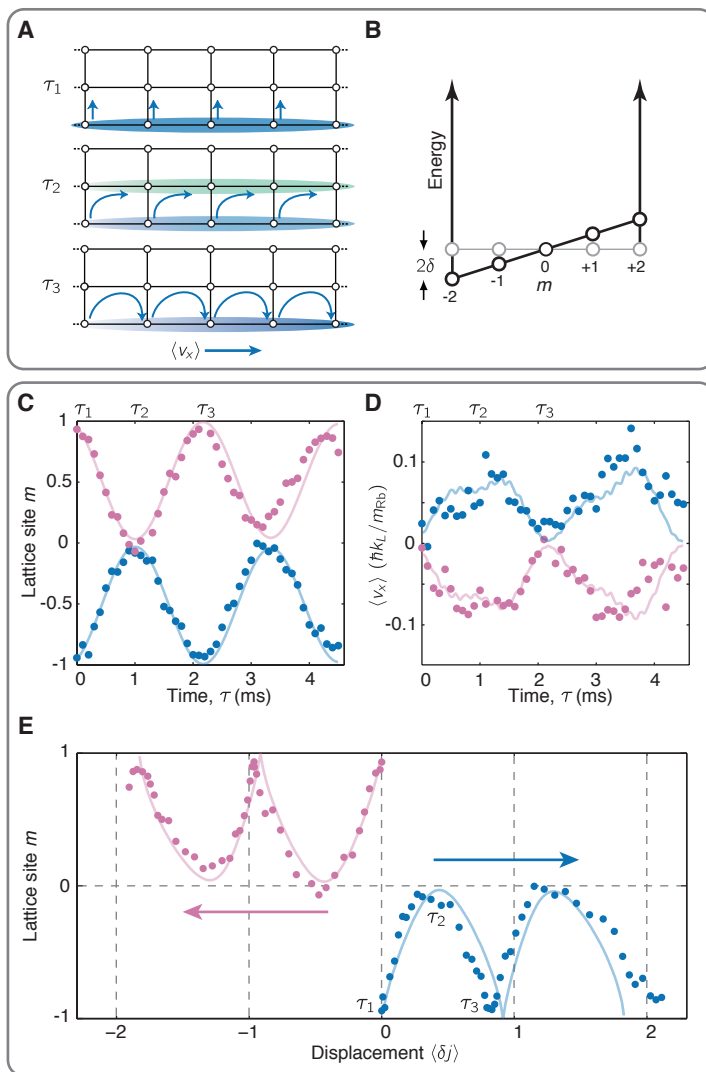


Figure 3:

Bibliography

- [1] K. v. Klitzing, G. Dorda, and M. Pepper. New method for high-accuracy determination of the fine-structure constant based on quantized hall resistance. *Phys. Rev. Lett.*, 45:494–497, Aug 1980.
- [2] D. J. Thouless, M. Kohmoto, M. P. Nightingale, and M. den Nijs. Quantized hall conductance in a two-dimensional periodic potential. *Phys. Rev. Lett.*, 49:405–408, Aug 1982.
- [3] Douglas R. Hofstadter. Energy levels and wave functions of bloch electrons in rational and irrational magnetic fields. *Phys. Rev. B*, 14:2239–2249, Sep 1976.
- [4] M. C. Geisler, J. H. Smet, V. Umansky, K. von Klitzing, B. Naundorf, R. Ketzmerick, and H. Schweizer. Detection of a landau band-coupling-induced rearrangement of the hofstadter butterfly. *Phys. Rev. Lett.*, 92:256801, Jun 2004.
- [5] B. Hunt, J. D. Sanchez-Yamagishi, A. F. Young, M. Yankowitz, B. J. LeRoy, K. Watanabe, T. Taniguchi, P. Moon, M. Koshino, P. Jarillo-Herrero, and R. C. Ashoori. Massive Dirac Fermions and Hofstadter Butterfly in a van der Waals Heterostructure. *Science*, 340:1427, 2013.

- [6] P. Zoller D. Jaksch. Creation of effective magnetic fields in optical lattices: the hofstadter butterfly for cold neutral atoms. *New Journal of Physics*, 5(1):56, 2003.
- [7] M. Aidelsburger, M. Atala, M. Lohse, J. T. Barreiro, B. Paredes, and I. Bloch. Realization of the hofstadter hamiltonian with ultracold atoms in optical lattices. *Phys. Rev. Lett.*, 111(18):185301–, October 2013.
- [8] Hirokazu Miyake, Georgios A. Siviloglou, Colin J. Kennedy, William Cody Burton, and Wolfgang Ketterle. Realizing the harper hamiltonian with laser-assisted tunneling in optical lattices. *Phys. Rev. Lett.*, 111:185302, Oct 2013.
- [9] Gregor Jotzu, Michael Messer, Remi Desbuquois, Martin Lebrat, Thomas Uehlinger, Daniel Greif, and Tilman Esslinger. Experimental realization of the topological haldane model with ultracold fermions. *Nature*, 515(7526):237–240, Nov 2014.
- [10] M Aidelsburger, M Lohse, C Schweizer, M Atala, J T Barreiro, S Nascimbène, N. R. Cooper, I. Bloch, and N. Goldman. Measuring the Chern number of Hofstadter bands with ultracold bosonic atoms. *Nature Physics*, 11(2):162–166, December 2014.
- [11] M. Mancini, G. Pagano, G. Cappellini, L. Livi, M. Rider, J. Catani, C. Sias, P. Zoller, M. Inguscio, M. Dalmonte, and L. Fallani. Observation of chiral edge states with neutral fermions in synthetic hall ribbons. *Science*, 349(6255):1510–, Sep 2015.
- [12] M Hafezi, S Mittal, J Fan, A Migdall, and J M Taylor. Imaging topological edge states in silicon photonics. *Nat. Photon.*, 7(12):1001–1005, October 2013.

- [13] A. Celi, P. Massignan, J. Ruseckas, N. Goldman, I.B. Spielman, G. Juzeliunas, and M. Lewenstein. Synthetic gauge fields in synthetic dimensions. *Phys. Rev. Lett.*, 112(4):043001–, Jan 2014.
- [14] B. K. Stuhl, H.-I. Lu, L. M. Ayccock, D. Genkina, and I. B. Spielman. Visualizing edge states with an atomic bose gas in the quantum hall regime. *Science*, 349(6255):1514–, Sep 2015.
- [15] Y. Aharonov and D. Bohm. Significance of electromagnetic potentials in quantum theory. *Phys. Rev.*, 115:485, 1959.
- [16] Yakir Aharonov and Ady Stern. Origin of the geometric forces accompanying berry’s geometric potentials. *Phys. Rev. Lett.*, 69(25):3593–3597, 1992.